



**HAL**  
open science

## Workspace, Joint space and Singularities of a family of Delta-Like Robot

Ranjan Jha, Damien Chablat, Luc Baron, Fabrice Rouillier, Guillaume Moroz

► **To cite this version:**

Ranjan Jha, Damien Chablat, Luc Baron, Fabrice Rouillier, Guillaume Moroz. Workspace, Joint space and Singularities of a family of Delta-Like Robot. *Mechanism and Machine Theory*, 2018, 127, pp.73-95. 10.1016/j.mechmachtheory.2018.05.004 . hal-01796066

**HAL Id: hal-01796066**

**<https://hal.science/hal-01796066>**

Submitted on 19 May 2018

**HAL** is a multi-disciplinary open access archive for the deposit and dissemination of scientific research documents, whether they are published or not. The documents may come from teaching and research institutions in France or abroad, or from public or private research centers.

L'archive ouverte pluridisciplinaire **HAL**, est destinée au dépôt et à la diffusion de documents scientifiques de niveau recherche, publiés ou non, émanant des établissements d'enseignement et de recherche français ou étrangers, des laboratoires publics ou privés.

# Workspace, Joint space and Singularities of a family of Delta-Like Robot

Ranjan Jha<sup>a</sup>, Damien Chablat<sup>b,\*</sup>, Luc Baron<sup>c</sup>, Fabrice Rouillier<sup>d</sup>, Guillaume Moroz<sup>e</sup>

<sup>a</sup>*BioMedical Instrumentation Division, CSIR- Central Scientific Instruments Organisation, Chandigarh, India*

<sup>b</sup>*Laboratoire des Sciences du Numérique de Nantes, UMR CNRS 6004, Nantes, France.*

<sup>c</sup>*Department of Mechanical Engineering, École Polytechnique de Montréal, Québec, Canada*

<sup>d</sup>*INRIA Paris-Rocquencourt, Institut de Mathématiques de Jussieu, UMR CNRS 7586, Paris, France.*

<sup>e</sup>*INRIA Nancy-Grand Est, Nancy, France.*

---

## Abstract

This paper presents the workspace, the joint space and the singularities of a family of delta-like parallel robots by using algebraic tools. The different functions of SIROPA library are introduced, which is used to induce an estimation about the complexity in representing the singularities in the workspace and the joint space. A Gröbner based elimination is used to compute the singularities of the manipulator and a Cylindrical Algebraic Decomposition algorithm is used to study the workspace and the joint space. From these algebraic objects, we propose some certified three-dimensional plotting describing the shape of workspace and of the joint space which will help the engineers or researchers to decide the most suited configuration of the manipulator they should use for a given task. Also, the different parameters associated with the complexity of the serial and parallel singularities are tabulated, which further enhance the selection of the different configuration of the manipulator by comparing the complexity of the singularity equations.

*Keywords:* Delta-like robot, Cylindrical algebraic decomposition, Workspace, Gröbner basis, Parallel robot, Singularities

---

---

\*. Corresponding author

*Email addresses:* [Ranjan.Jha@csio.res.in](mailto:Ranjan.Jha@csio.res.in) (Ranjan Jha), [Damien.Chablat@cnrs.fr](mailto:Damien.Chablat@cnrs.fr) (Damien Chablat), [Luc.Baron@polymtl.ca](mailto:Luc.Baron@polymtl.ca) (Luc Baron), [Fabrice.Rouillier@inria.fr](mailto:Fabrice.Rouillier@inria.fr) (Fabrice Rouillier), [Guillaume.Moroz@inria.fr](mailto:Guillaume.Moroz@inria.fr) (Guillaume Moroz)

## Nomenclature

SIROPA	Library for manipulator singularities analysis
CAD	Cylindrical Algebraic Decomposition
IKP	Inverse Kinematics problem
DKP	Direct Kinematics problem
det	Determinant of Jacobian matrix
R	Revolute Joint
P	Prismatic Joint
S	Spherical Joint
$\rho$	Actuated Joint Variables
X	Pose Variables
<b>A</b>	Direct parallel Jacobian matrices
<b>B</b>	Inverse serial Jacobian matrices

## 1. Introduction

The workspace can be defined as the volume of space or the complete set of poses which the end-effector of the manipulator can reach. Many researchers published several works on the problem of computing these complete sets for robot kinematics. Based on the early studies [1, 2], several methods for workspace determination have been proposed, but many of them are applicable only to a particular class of robots. The workspace of parallel robots mainly depends on the actuated joint variables, the range of motion of the joints and the mechanical interferences between the bodies of the mechanism. There are different techniques based on geometric [3, 4], discretization [5, 6, 7], and algebraic methods [8, 9, 10, 11, 12] which can be used to compute the workspace of parallel robot. The main advantage of the geometric approach is that it establishes the nature of the boundary of the workspace [13]. Also, it allows to compute the surface and volume of the workspace while being very efficient in terms of storage space, but when the rotational motion is included, it becomes less efficient. Interval analysis based methods can be used to compute the workspace but the computation time depends on the complexity of the robot and the requested accuracy [7]. Discretization methods are usually less complicated and can easily take into account all kinematic constraints, but they require more space and computation time for higher resolutions. The majority of numerical methods used to determine the workspace of parallel manipulators includes the discretization of the pose parameters for computing workspace boundaries [6]. There are other approaches, such that optimization algorithms [14] for fully serial or parallel manipulators; analytic methods for symmetrical spherical mechanisms [15]. In [16], a method for computing the workspace boundary for manipulators with a general structure is proposed, which uses a branch-and-prune technique to isolate a set of output singularities, and then classifies the points on such set according to whether they correspond to motion impediments in the workspace. A Cylindrical Algebraic Decomposition (CAD) based method is used in [10, 17, 18] to model the workspace and joint space for the 3-RPS parallel robot and delta-like robots. The variations in the workspace, singularities, and joint space with respect to design parameter of a 3-RPS parallel manipulator is studied in [19].

Here, this paper presents the results obtained by applying algebraic methods for the workspace and joint space analysis of a family of a delta-like robot including complexity information for representing the singularities in the workspace and the joint space. The CAD algorithm is used to study both the workspace and joint space, and a Gröbner based elimination process is used to compute the parallel and serial singularities of the manipulator. The structure of the paper is as follows. Section 2 presents the mathematical tools and the introduction of SIROPA. Section 3 describes the architecture of the manipulator, including kinematic equation and joint constraints associated with the manipulators. Section 4 discusses the computation of parallel as well as serial singularities and their projections in workspace and joint-space. Section 5 and 6 present a comparative study on the shape of the workspace and joint space of different delta-like robots, respectively. Section 7 finally concludes the paper.

## 2. Algebraic Tools : SIROPA

SIROPA is a library for the MAPLE developed to analyze the singularities, workspace and joint space of serial and parallel manipulators as well as tensegrity structures [20]. There are two main parts of the library shown in Fig.(1), the first one provides the algebraic tools to solve the constraint equations and convert the trigonometric equations in the algebraic form. The other one, SIROPA, provides modeling, analyzing and plotting functions for different manipulators, shown in Fig.(2). Only a small part of these tools are used in the current paper.

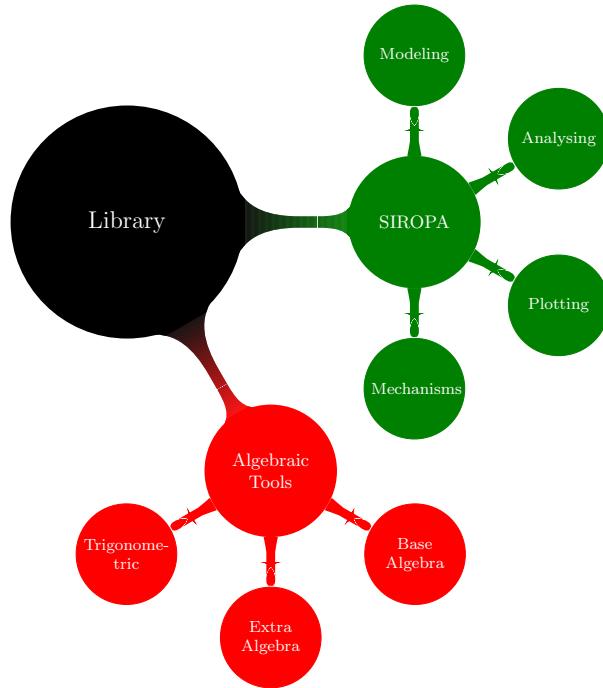


FIGURE 1: Architecture of Library

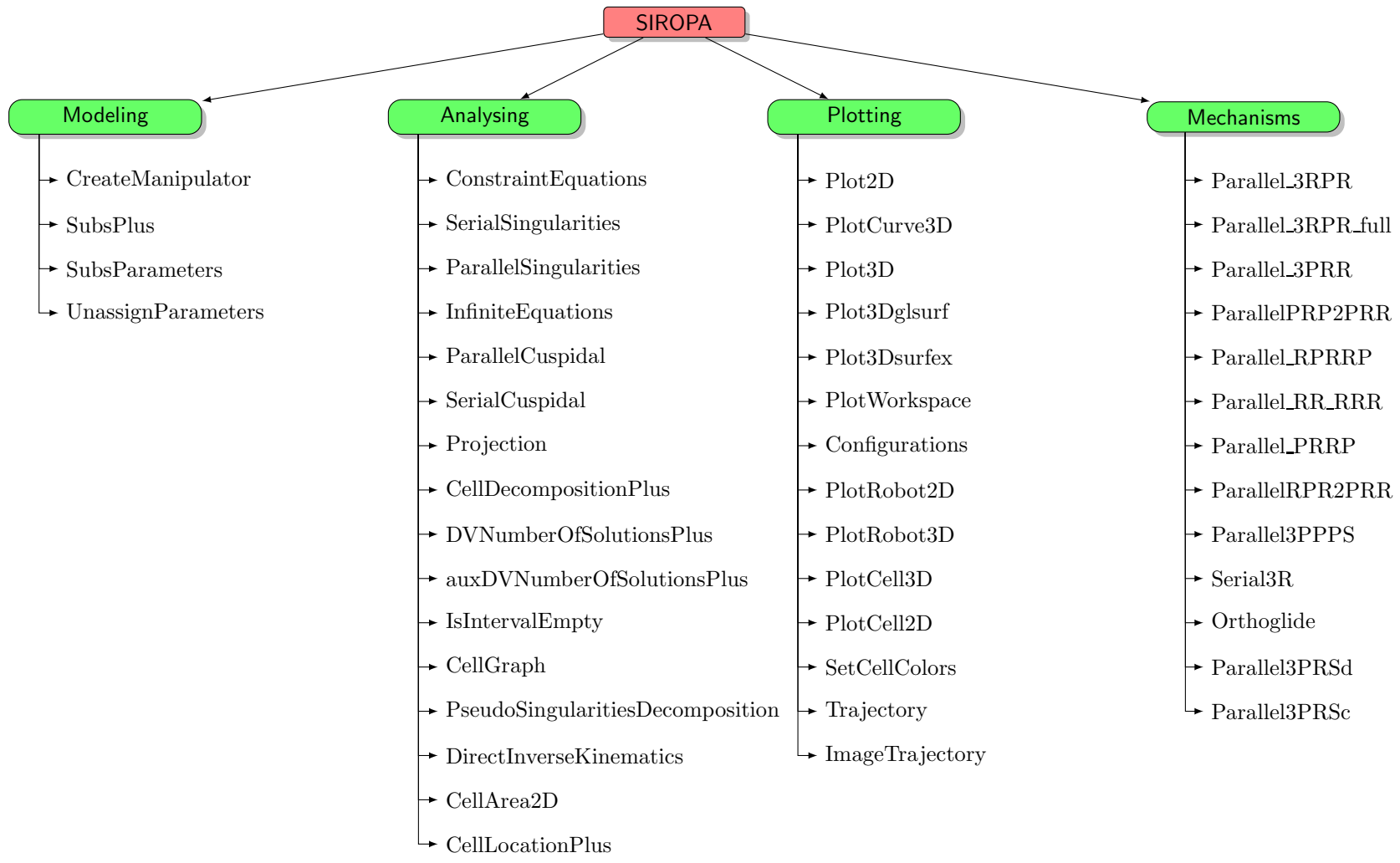


FIGURE 2: List of all the defined functions in SIROPA library

## 2.1. Modeling Functions

SIROPA provides modeling functions such as `CreateManipulator()`, to virtually create the planar and spatial manipulators for further analysis. Below are the functions :

### Functions

<code>CreateManipulator</code>	Constructs a data structure of type <code>Manipulator</code>
<code>SubsPlus</code>	Substitute coherently angles in a system
<code>UnassignParameters</code>	Specify parameter values in a <code>Manipulator</code>
<code>UnassignParameters</code>	Release parameters in a <code>Manipulator</code>

60

## CreateManipulator

The function `CreateManipulator()` of SIROPA library in MAPLE software is used to virtually create the manipulator for analysis. Listing 1 shows the code architecture of the function.

65

As shown in Listing 1, compulsory inputs are identified as `[c]`, while the optional ones as `[o]`. `Points`, `loops`, `chains` and `actuators`, are the input parameters to create the plot of the manipulator. The pose variables are the essential input parameters to define the mechanism. The input parameter `sys` is the set of constraint equations associated with the motion of manipulator.

70

```

1 CreateManipulator := proc (
2   sys[c]      :: list({algebraic, algebraic=algebraic, algebraic<
   algebraic})
3   cart[c]     :: list(name),
75 4   arti[c]     :: list(name),
5   passive[o]  :: list(name),
6   geompars[c]:: list(name),
7   spec[o]     :: {list, set}(name=algebraic),
8   plotrange[o]:: list(name=range),
80 9   points[p]  :: list(name=list(algebraic)),
10  loops[p]   :: list(list(name)),
11  chains[p]  :: list(list(name)),
12  actuators[p]:: list({list(name), name}),
13  model[o]   :: string                := "No name",
85 4   precision[o]:: integer            := 4,
15  {
16  noradical  :: truefalse            := false
17  }
18 )

```

Listing 1: Architecture of Create Manipulator

90 Constructs a data structure of type `Manipulator`.

This function returns a data structure of type `Manipulator` containing the fields, briefly described below. Further, the values of these fields can be retrieved or changed according to the analysis to be performed.

## Parameters

sys	list of polynomials, polynomial equalities and polynomial inequalities with rational coefficients : the implicit equations and constraints of the considered manipulator
cart	list of names : the pose variables
arti	list of names : the control parameters; default value : the names of <code>sys</code> not in <code>vars</code>
passive	list of names : the passive variables; default value : []
geomparams	list of names : the geometric parameters; default value : the names of <code>sys</code> not in <code>cart</code> , nor in <code>arti</code>
spec	a list of equations of the form name=formula where name is a parameter name and formula a polynomial with trigonometric function ; the new variables in a formula are handled in the same way as the replaced variable. default value : []
points	list of name=list : the points of the robot with their coordinates; default value : []
loops	list of list of names : the frame loops of the robot default value : []
chains	list of list of names : the frame chains of the robot default value : []
actuators	list of names or list of names : the robot actuators; a list of name is for a leg actuator, a name is for an angle actuator; default value : []
model	string : the name of the model; default value : No name
precision	an integer : the number of significative digits; default value : 4

## Remarks

- 95 — Polynomials `p` appearing in `sys`, `Equations`, `GenericEquations` are considered implicitly as `p=0`.
- When a control parameter value is specified in `spec`, the parameter name is removed from the `ControlParameters` field. This is not the case for the geometric parameters that appears in the field `GeometricParameters`
- 100 even if they are specified.

### 2.2. Analysing Functions

SIROPA provides the analysing function to compute the parallel and serial singularities. These functions are used to study both the workspace and joint space. The architecture of `ConstraintEquations` and `CellDecompositionPlus` are shown in Listing 2 and 3.

105

## ConstraintEquations

```
1 ConstraintEquations := proc ( robot :: Manipulator ,  
2 {  
3 constraints :: truefalse := false  
4 }
```

## Returns

Equations	a list of polynomials $[p_1, \dots, p_k]$ : the modeling equations
Constraints	a list of strict inequalities : the constraint inequalities
ArticularVariables	a list of names : the control parameters
PassiveVariables	a list of names : the remaining variables
GeometricParameters	a list of names : the geometric parameters
GenericEquations	a list of polynomials : the modeling equations with symbolic geometric parameters
GenericConstraints	a list of strict inequalities : the constraint inequalities appearing in sys
Precision	an integer : the number of correct digits
PoseValues	the pose values substituted in the <a href="#">GenericEquations</a> to get the Equations
ArticularValues	the articular values substituted in the <a href="#">GenericEquations</a> to get the Equations
PassiveValues	the passive values substituted in the <a href="#">GenericEquations</a> to get the Equations
GeometricValues	the geometric values substituted in the <a href="#">GenericEquations</a> to get the Equations
DefaultPlotRanges	ranges used by default for plotting if provided
Points	the points coordinate of the robot
Loops	the frame loops of the robot
Chains	the frame chain of the robot
Actuators	the actuators of the robot
Model	a string : the name of the modeling

5 )

Listing 2: Architecture of ConstraintEquations function

Computes the implicit equations induced by the constraints.

## Parameters

robot a data structure returned by a function mechanisms.

## 115 Returns

A list of list of polynomials : each list represents a component of the equations satisfied by the constraints.

## CellDecompositionPlus

```
1 CellDecompositionPlus := proc ( equ :: list(algebraic),
120 2     ineq :: list(algebraic),
3     vars :: list(name),
4     pars :: list(name) := [ op(indets([equ,
5     ineq],name) minus {op(vars)}) ],
6     {
125 7     nofactor :: truefalse := false,
8     gbfactor :: truefalse := false,
9     norealrootstest :: truefalse := false
10 }
}
```



## Functions

ConstraintEquations	Computes the implicit equations induced by the constraints.
SerialSingularities	Computes the implicit equations satisfied by the singularities.
ParallelSingularities	Computes the implicit equations satisfied by the singularities.
InfiniteEquations	Computes the equations where the manipulator has infinitely many solutions.
ParallelCuspidal	Computes the implicit equations satisfied by the cuspidal points.
SerialCuspidal	Computes the implicit equations satisfied by the cuspidal points.
Projection	Project on variables or expressions in a polynomial system.
CellDecompositionPlus	Describes the parameter space according to the number of real roots.
NumberOfSolutionsPlus	Returns the number of real solutions of cells obtained by <a href="#">CellDecompositionPlus</a> .
DVNumberOfSolutionsPlus	Returns the number of real solutions on the intersection points of the Discriminant Variety.
auxDVNumberOfSolutionsPlus	Auxiliary function Returns the number of real solutions on the intersection points of the Discriminant Variety.
IsIntervalEmpty	Checks that a polynomial has no real roots in an open interval.
CellGraph	Computes the connexity graph of the cells of a CAD.
DirectInverseKinematics	Returns the cells having the same antecedent.
CellArea2D	Compute the area of the cells returned <a href="#">CellDecomposition</a> or <a href="#">CellDecompositionPlus</a> .
CellLocationPlus	Computes the cells of a decomposition containing the given points.

11

Listing 3: Architecture of CellDecompositionPlus function

130 Describes the parameter space according to the number of real roots.

## Returns

A maple object : the same as the one returned by the maple function `RootFinding[Parametric][CellDecomposition]`. The main difference is that it handles trigonometric expressions.

## Parameters

equ	a list of polynomials and trigonometric expressions : the equations.
ineq	a list of polynomials and trigonometric expressions : the inequalities where each expression p stands for $p > 0$ .
vars	a list of names : the variables of the system
pars	a list of names : the parameters of the system; default value : the remaining variables of <a href="#">equ</a> and <a href="#">ineq</a>

### 135 2.3. Plotting Functions

These functions are used to plot the workspace, joint space and singularity surfaces. Listing 4, 5, 6 and 7 shows the architecture of Plot2D, Plot3D, Configurations and PlotRobot3D, respectively.

#### Functions

Plot2D	Plots a system of 2 variables
PlotCurve3D	Plots a curve given by implicit equations in 3 variables
Plot3D	Plots a system of 3 variables using maple internal plotting functions
Plot3Dglsurf	Plots a system of 3 variables using glsurf
Plot3Dsurfex	Plots a system of 3 variables using surfex (software based on surf)
PlotWorkspace	Plot the border of a manipulator workspace
Configurations	Computes the different possible positions
PlotRobot2D	Plot a planar manipulator
PlotRobot3D	Plot a 3D manipulator
PlotCell3D	Plot the cells returned CellDecomposition or CellDecompositionPlus
PlotCell2D	Plot the cells returned CellDecomposition or CellDecompositionPlus
SetCellColors	Set colors to the numbers of solutions obtained by NumberOfSolutionsPlus
Trajectory	Display a given trajectory
ImageTrajectory	Display a given trajectory

#### Plot2D

```

140 1 Plot2D := proc (
2     sys ::{ algebraic , equation(algebraic) , list({ algebraic ,
3     equation(algebraic) , algebraic<algebraic} ) , list(list({
4     algebraic , equation(algebraic) , algebraic<algebraic} ) ) } ,
5     e1 ::name = range ,
145 6     e2 ::name = range ,
7     {
8     points ::truefalse := false ,
9     [ notest , draft ] ::truefalse := false
10    }
150 1 )

```

Listing 4: Architecture of Plot2D function

Plots a system of 2 variables.

### Parameters

**sys** a list or a list of list of polynomials : the system  
**v1 = r1** v1 is a name of sys and r1 a range of values  
**v2 = r2** v2 is a name of sys and r2 a range of values  
**points = bool** bool is a boolean : if false, isolated points are ignored;  
 default value : false;  
**notest = b** b is a boolean; when b is true the inequality and real  
 constraints are ignored; default value : true;  
**opts** arguments passed to the maple function plots :-  
 implicitplot

### Returns

A graphic : the solutions of the system,  
 — when **sys** is a list of polynomials [p1,...,pk], the graphic is the zeroes of  
 the system p1=0 and ... and pk=0  
 — When **sys** is a list of list of polynomials [L1,...,Lk], the graphic is the  
 union of the zeroes of each system L1, ..., Lk.

```

Plot3D
1 Plot3D := proc (
160 2   sys :: { algebraic, equation(algebraic), list({ algebraic,
3     equation(algebraic), algebraic<algebraic}), list(list({
4     algebraic, equation(algebraic), algebraic<algebraic}))},
5     ineq :: list({polynom, polynom<polynom}) := [],
6     e1 :: name = range := sort ([op(indets([sys,x,y,z],
165 7     name))] [1] = -5..5,
8     e2 :: name = range := sort ([op(indets([sys,x,y,z],
9     name) minus {lhs(e1)}))] [1] = -5..5,
10    e3 :: name = range := sort ([op(indets([sys,x,y,z],
11    name) minus {lhs(e1),lhs(e2)}))] [1] = -5..5,
170 2    {
13      points :: truefalse := false,
14      crossingrefine :: truefalse := false,
15      grid :: integer := 10,
16      border :: constant := 10^(-30),
175 7      output :: identical(list, display) := '-display'
18    }
19  )
  
```

Listing 5: Architecture of Plot3D function

Plots a system of 3 variables using maple internal plotting functions.

### Returns

A graphic : the solutions of the system,  
 — when **sys** is a polynomial, the graphic is the zeroes of this polynomial  
 — when **sys** is a list of polynomials [p1,...,pk], the graphic is the zeroes of  
 the system p1=0 and ... and pk=0  
 — when **sys** is a list of list of polynomials [L1,...,Lk], the graphic is the union  
 of the zeroes of each system L1, ..., Lk.

## Parameters

sys	a list or a list of list of polynomials : the system
v1 = r1	v1 is a name of sys and r1 a range of values
v2 = r2	v2 is a name of sys and r2 a range of values
v3 = r3	v3 is a name of sys and r3 a range of values
points = bool	bool is a boolean : if false, isolated points are ignored; default value : false;
grid = i	i is an integer leading to a grid size i x i; default value : 20.
border = e	e is a numeric value : defines the precision on the border; default value : 0.0001.
crossingrefine = bool	bool is a boolean : if true, the mesh follows the cross of the different surfaces; default value : false.
output = keyword	keyword is either list or display : display (resp. list) returns a graph (resp. a list).

## Configurations

This function computes the different possible working modes for given values of pose variables and assembly modes for given values of articular variables.

```
1 Configurations := proc ( robot  :: Manipulator ,  
190 2     spec    :: seq (name=constant) ,  
3     {  
4     noconstraints  :: truefalse  := false ,  
5     ordering      :: name      := NULL  
6     }  
    )
```

Listing 6: Architecture of Configuration function

195 Computes the different possible positions.

## Parameters

robot	an object of type Manipulator
spec	sequence of name=constant : the specification of the known variables (the articular values or the pose values, or other)
noconstraints=*b*	b is a boolean : when true, the constraint inequalities are ignored; default value : false.
ordering	ordering is a name used to order the solutions; default value : NULL

## Returns

A list of elements : each elements is a list of name=list(constant) and represents a configuration of the input manipulator.

## PlotRobot3D

200 The PlotRobot3D function is used to plot any possible configuration of a manipulator, which helps in visualizing the manipulator in three-dimensional space.

```
1 PlotRobot3D := proc (
2     robot    :: Manipulator ,
3     spec    :: seq(name=constant) ,
4     k      :: { integer , range , list ( integer ) } := .. ,
5     {
6     color := [] ,
7     legendvars := subs (map(s->lhs(s)=NULL,[spec]) ,
210 8     [op(robot:-ArticularVariables) , op(robot:-
PoseVariables) ,
9     op(robot:-PassiveVariables) , 'det(J)']) ,
10     nolegend :: truefalse := false ,
11     noconstraints :: truefalse := false
215 2     }
13 )
```

Listing 7: Architecture of PlotRobot3D function

Computes the different possible positions.

### Parameters

robot	a Manipulator : the 3D robot to plot
spec	a sequence of name=constant : specification of variables of the robot to plot
k	an integer : specifies one of the possible configuration when several are available
color=col	equation of the shape color=*col*, where col is a color or a list of colors; when the number of specified color is not enough, deterministic colors are chosen; default value : empty list.
legendvars	list of names : the variables to display in the legend ; default value : the articular, passive and pose variables, minus the variables in spec
nolegend=b	b is a boolean : when false, a legend is displayed (the graphic appears in a separate windows with a classic worksheet); default value : false.

### Returns

220 A graphic : the different configurations of the manipulator satisfying the input specifications.

#### 2.4. Mechanisms Functions

There are some manipulators like 3-RPR (see Listing 8), 3-PRR, RPRRP, 3-PPPS, Orthoglide, 3-PPPS and 3-PRS which are predefined in SIROPA library, and can be accessible using these functions [21, 22, 23, 24].

## Functions

Parallel3RPR	Constructs the Manipulator object of planar 3-R <u>P</u> R
Parallel3RPR_full	Constructs the Manipulator object of planar 3-R <u>P</u> R
Parallel3PRR	Constructs the Manipulator object of a 3- <u>P</u> RR
ParallelPRP2PRR	Constructs the Manipulator object of a PRP2PRR
ParallelRPRRP	Constructs the Manipulator object of a R <u>P</u> RR <u>P</u>
ParallelRR_RRR	Constructs the Manipulator object of a 2-RR
ParallelPRRP	Constructs the Manipulator object of a <u>P</u> RR <u>P</u>
Orthoglide	Constructs the Manipulator object of Orthoglide
ParallelRPR2PRR	Constructs the Manipulator object of the RPR2PRR
Parallel3PPPS	Constructs the Manipulator object of the 3- <u>P</u> PPS
Serial3R	Constructs the Manipulator object of the serial 3R manipulator.
Parallel3PRSc	Constructs the Manipulator object of the 3- <u>P</u> RS
Parallel3PRSc	Constructs the Manipulator object of the 3- <u>P</u> RS

## 225 Parallel3RPR

```

1 Parallel3RPR := proc( {
2     d1  :: algebraic := 17.04,
3     d2  :: algebraic := 16.54,
4     d3  :: algebraic := 20.84,
230 5     beta :: algebraic := arccos ((d2^2-d3^2-
6     d1^2)/(-2*d3*d1)),
7     A2x  :: algebraic := 15.91,
8     A3x  :: algebraic := 0,
9     A3y  :: algebraic := 10,
235 0     precision :: integer := 4
11     }
12     ,
13     morespec  :: seq(name=algebraic) ,
14     moreranges :: seq(name=range)
)

```

Listing 8: Architecture of Parallel3RPR function

240 Constructs the Manipulator object of a planar 3-RPR manipulator.

## Parameters

name = constant	<p>the geometric parameters of the robot (see Fig.(3)),</p> <ul style="list-style-type: none"> <li>— where name is one of d1, d2, d3, beta, A2x, A3x, A3y,</li> <li>— All the variables d1, d3, A2x, A3x, A3y must be assigned.</li> <li>— One of d2, beta must be assigned (if both are assigned, d3 is ignored).</li> <li>— By default, the values are d1 = 17.04, d2 = 16.54, d3 = 20.84, A2x = 15.91, A3x = 0, A3y = 10.</li> </ul>
precision = integer	<p>the precision, where integer is the number of significant digits; default value : 4.</p>

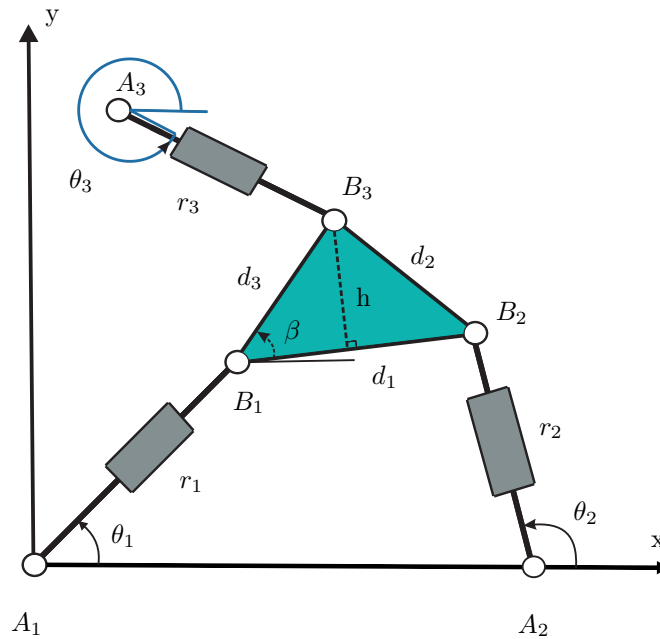


FIGURE 3: 3-RPR parallel robot

### Returns

A Manipulator data structure representing the planar 3-RPR manipulator whose dimensions are given in input.

### 2.5. Standard Bases (Gröbner Bases)

245 The method of Gröbner bases provides a uniform approach to solve a wide range of problems expressed in terms of sets of multivariate polynomials. The Gröbner basis gives us a method for writing a system of algebraic equations  $f(x_1, \dots, x_n) = 0$  in terms of unknowns  $x_1, \dots, x_n$  with finitely many solutions into a system that has the same roots and in a triangular form  $g_n(x_n) =$   
 250  $0, g_{n-1}(x_{n-1}, x_n) = 0, \dots, g_1(x_1, \dots, x_n) = 0$ , called a Gröbner basis. There are few drawbacks of Gröbner basis such that the calculation time of the Gröbner basis is mainly dependent upon the number of equations and their degree; while its calculation with real numbers is numerically unstable [25].

Gröbner basis theory can be used to compute the projections  $\pi_Q$  and  $\pi_W$   
 255 into the joint space and the workspace, respectively. Let  $P$  be a set of polynomials in the variables  $X = (x_1, \dots, x_n)$  and  $q = (q_1, \dots, q_n)$ . Moreover, let  $V$  be the set of common roots of the polynomial in  $P$ , let  $W$  be the projection of  $V$  on the workspace and  $Q$  the projection on the joint space. It might not be possible to represent  $W$  (resp.  $Q$ ) by polynomial equations. Let  $\bar{W}$  (resp.  $\bar{Q}$ ) be the smallest  
 260 set defined by polynomial equations that contain  $W$  (resp.  $Q$ ) [11]. A Gröbner basis  $P$  is a polynomial system equivalent to  $P$ , satisfying some additional specific properties. The Gröbner basis of a system depends on the chosen ordering of monomials.

For the projection  $\pi_Q$ , when we choose an ordering eliminating  $\mathbf{q}$ , the Gröbner  
 265 basis of  $P$  contains exactly the polynomials defining  $\bar{W}$ .

sys	list of equations and strict inequalities between polynomials with rational coefficients
vars	list of names ; the indeterminates
pars	(optional) list of names ; the parameters
eqs	list of polynomials $f$ with rational coefficients, representing equations of the form $f = 0$
ineqs	list of polynomials $g$ with rational coefficients, representing constraint inequalities of the form $0 < g$

TABLE 1: Description of the fields of DiscriminantVariety function

For the projection  $\pi_W$ , when we choose an ordering eliminating  $\mathbf{X}$ , the Gröbner basis of  $P$  contains exactly the polynomials defining  $\bar{Q}$ .

### 2.6. Discriminant Variety and Cylindrical Algebraic Decomposition

270 The notion of discriminant variety is a generalization of the discriminant of a univariate polynomial, describing all the critical points of a system, including singularities, solutions of multiplicity greater than one, and solutions at infinity. It is a subset of the parameter space of lower dimension [26, 27].

275 As shown in Table 1, a discriminant variety has the following property : it divides the parameter space into open, full-dimensional cells such that the number of solutions of the system `sys` is constant for parameter values chosen from the same open cell. As shown in Listing 9, the function `DiscriminantVariety(sys, vars, pars)` computes a discriminant variety of the system `sys` of equations and inequalities with respect to the indeterminates `vars` and the parameters `pars`.

```
280 1 DiscriminantVariety (sys, vars, pars)
2 DiscriminantVariety (eqs, ineqs, vars, pars)
```

Listing 9: Architecture of Discriminant Variety

The function `DiscriminantVariety(eqs, ineqs, vars, pars)` computes a discriminant variety of the system

$$[f = 0, 0 < g]_{f \in eqs, g \in ineqs} \quad (1)$$

of equations and inequalities with respect to the indeterminates `vars` and the parameters `pars`.

The input system must satisfy the following properties :

- 285 — There are at least as many equations as indeterminates.
- At least one and at most finitely many complex solutions exist for almost all complex parameter values (the system is generically solvable and generically zero-dimensional).
- 290 — For almost all complex parameter values, there are no solutions of multiplicity greater than one (the system is generically radical). In particular, the input equations are square-free.

An error occurs if one of these three previous conditions is violated.



- The result is returned as a list of lists of polynomials in `vars` such that the discriminant variety is the union of the set of solutions of the polynomials in each inner list.
- If `vars` is not specified, it defaults to all the names in `sys` that are not indeterminates.
- This function attempt to find a minimal discriminant variety, but it may return a proper superset in the case that it does not succeed.
- The discriminant variety is computed using Gröbner basis techniques.

*Example 1*

```

1 with( RootFinding [ Parametric ] )
2 DiscriminantVariety[ a*x^2=1, b*z+y=0, c*z+y=0, 0 < c ], [ x, y, z ]
3
305 4 Output [[ a ], [ c ], [ b-c ]]

```

Listing 10: Example of Discriminant Variety

The discriminant variety in Listing 10 is  $(a, b, c) : a = 0$  **or**  $b = c$  **or**  $c = 0$ . The case  $a = 0$  gives a solution of the first equation at infinity. In the case  $b = c$ , the second and third equations coincide and therefore the system becomes underdetermined and has infinitely many solutions. Finally, the case  $c = 0$  corresponds to a boundary case for the inequality  $0 < c$ .

A cylindrical algebraic decomposition of the  $n$ -dimensional real space is a partition of the whole space into connected semi-algebraic subsets such that the cells in the partition are cylindrically arranged, that is, the projection of any two cells onto any lower dimensional real space is either equal or disjoint. This decomposition is called **F**-invariant if, for any given cell, the sign of each polynomial in **F** does not change over the cell. `CylindricalAlgebraicDecompose(F, R)` returns an **F**-invariant CAD of the  $n$ -dimensional real space, where  $n$  is the number of variables in **R**. This assumes that **R** has characteristic zero and no parameters, such that the base field of **R** is the field of rational numbers [28].

The output of `CylindricalAlgebraicDecompose(F, R)` has several possible formats controlled by the options `output = piecewise, tree, list, cadcell, rootof`. In all formats, each cell provides at least two pieces of information; the index of the cell; and a sample point of the cell. In the `cadcell` and `rootof` output formats, a defining semi-algebraic system (called a Tarski Formula) is also provided. Due to the cylindricity property, cells can be organized in a hierarchical manner. This is the purpose of `piecewise` and `tree` output format, whereas the other three formats are flat representations. Due to the potentially large number of cells, the `cadcell` format only shows the name `cadcell` for each cell in the decomposition. However, `cadcell` is a type and an object of that type can be passed to `Display`. It can also be passed to `SamplePoints` in order to access the sample point of the cell. The `rootof` format is meant to be compatible with the output format of the `solve` command.

As shown in Listing 11 and Table 2, the `CellDecomposition` function decomposes the parameter space of a parametric polynomial system into cells in which the original system has a constant number of solutions [29].

sys	list of equations and strict inequalities between polynomials with rational coefficients
vars	list of names; the indeterminates
pars	(optional) list of names; the parameters
eqs	list of polynomials $f$ with rational coefficients, representing equations of the form $f = 0$
posineqs	list of polynomials $g$ with rational coefficients, representing constraint inequalities of the form $0 < g$
nzineqs	list of polynomials $g$ with rational coefficients, representing constraint inequations of the form $g \neq 0$
options	sequence of optional equations of the form keyword=value, where keyword is either output or method

TABLE 2: Description of the fields of CellDecomposition function

```

1 CellDecomposition (sys, vars, pars, options)
2 CellDecomposition (eqs, posineqs, vars, pars, options)
3 CellDecomposition (eqs, posineqs, nzineqs, vars, pars, options)

```

Listing 11: Architecture of Cell Decomposition

The function returns a data structure that can be used for (examples) :

- Plotting the regions of the parameter space for which the system has a given number of solutions.
- Extracting sample points in the parameter space for which the system has a given number of solutions.
- Extracting boxes in the parameter space in which the system has a given number of solutions.

The record returned captures information about the solutions of the system depending on the parameter values, including :

- a discriminant variety;
- for each full-dimensional open cell, a sample point strictly in the interior of the cell; if possible, the coordinates of the sample point are chosen to be integers.

The input system must satisfy the following properties :

- The number of equations is equal to or greater than the number of indeterminates;
- At most finitely many complex solutions exist for almost all complex parameter values (the system is generically zero-dimensional);
- For almost all complex parameter values, there are no solutions of multiplicity greater than one (the system is generically radical); in particular, the input equations are square-free.

### 3. Manipulators Under Study

There are four different mechanisms for which the workspace, the joint space and the singularities are presented in this paper. Three degree of freedom parallel mechanisms consisting of three identical legs, while the different arrangements of these legs give rise to family of delta like robot. Several types of delta-like robot were studied, few of them are Orthoglide [7, 30], Hybridglide, Triaglide

[31] and UraneSX [7]. The kinematic equations of the family of delta like robot can be generalized as  $\|\mathbf{P} - \mathbf{B}_i\| = L_i$ . These constraint equations can be in the form of Euler angle representation or quaternions [10]. All the computations and analysis are done for  $L_i = L = 2$  and by imposing the following constraints on joint variables. Without joint limits, the whole family of these robots admit two assembly modes and eight working modes, i.e. ,

$$0 < \rho_1 < 2L \quad 0 < \rho_2 < 2L \quad 0 < \rho_3 < 2L \quad (2)$$

### 3.1. Orthoglide Architecture and Kinematics

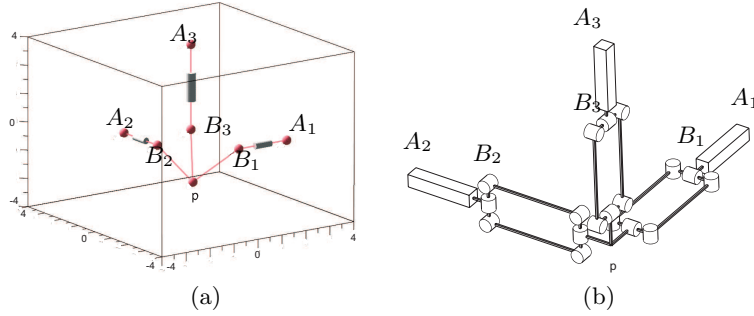


FIGURE 4: Configuration of Orthoglide : (a) simplified ; (b) real.

As shown in Fig.(4), the *Orthoglide* mechanism is driven by three actuated orthogonal prismatic joints. A simpler model can be defined for the Orthoglide, namely, three bar links connected by the revolute joints to the tool center point on one side and to the corresponding prismatic joint at another side. Several assembly modes of these robots depends upon the solutions of direct kinematic problem (DKP). The point  $\mathbf{P}$  represents the pose of corresponding robot. However, more than one position for the point  $\mathbf{P}$  shows the multiple solutions for the DKP.  $\mathbf{A}_i\mathbf{B}_i$  is equal to  $\rho_i$ , where  $\rho_i$  represents the prismatic joint variables, whereas  $\mathbf{P}$  represents the position vector of the tool center point. The constraint equations for the Orthoglide are :

$$\begin{aligned} (x - \rho_1)^2 + y^2 + z^2 &= L^2 \\ x^2 + (y - \rho_2)^2 + z^2 &= L^2 \\ x^2 + y^2 + (z - \rho_3)^2 &= L^2 \end{aligned} \quad (3)$$

The Maple lines used to describe this robot are as follows, shown in Listing 12

```

1 robot:= CreateManipulator (
2   [(rho1-x)^2+y^2+z^2-1^2,
375 3   (rho2-y)^2+x^2+z^2-1^2,
4     (rho3-z)^2+x^2+y^2-1^2,
5     rho1>0, rho2>0, rho3>0,
6     rho1<2*1, rho2<2*1, rho3<2*1],
7     [x, y, z],
380 8     [rho1, rho2, rho3],
9     [1=1],
10    [rho1=-15/10..15/10, rho2=-15/10..15/10,
11    x=-15/10..15/10, y=-15/10..15/10],

```

```

12 [A1 = [2*1, 0, 0], A2 = [0, 2*1, 0], A3 = [0, 0, 2*1],
385.3 M = [x, y, z],
14 B1 = [rho1, 0, 0], B2 = [0, rho2, 0], B3 = [0, 0, rho3]],
15 [],
16 [[B1, M], [B2, M], [B3, M]],
17 [[A1, B1], [A2, B2], [A3, B3]],
390.8 "Orthoglide");
19 )

```

Listing 12: Maple lines to create the Orthoglide robot

### 3.2. Hybridglide Architecture and Kinematics

As shown in Fig.(5), the *Hybridglide* mechanism consists of three actuated prismatic joints, in which two actuators are placed parallel and third one perpendicular to others two. Also the three bar links connected by spherical joints to the tool center point on one side and to the corresponding prismatic joint at another side. Several assembly modes of these robots depends upon the solutions of the DKP.

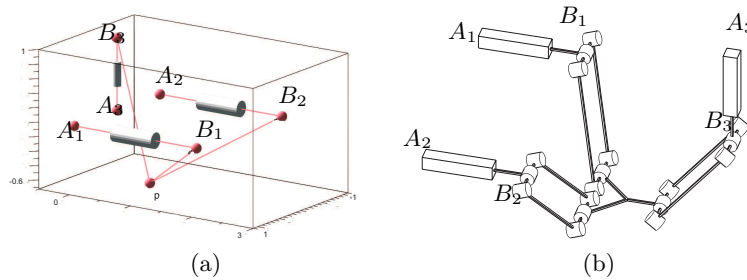


FIGURE 5: Configuration of Hybridglide : (a) simplified; (b) real.

The constraint equations for the Hybridglide are :

$$\begin{aligned}
 (x - 1)^2 + (y - \rho_1)^2 + z^2 &= L^2 \\
 (x + 1)^2 + (y - \rho_2)^2 + z^2 &= L^2 \\
 x^2 + y^2 + (z - \rho_3)^2 &= L^2
 \end{aligned} \tag{4}$$

### 400 3.3. Triaglide Architecture and Kinematics

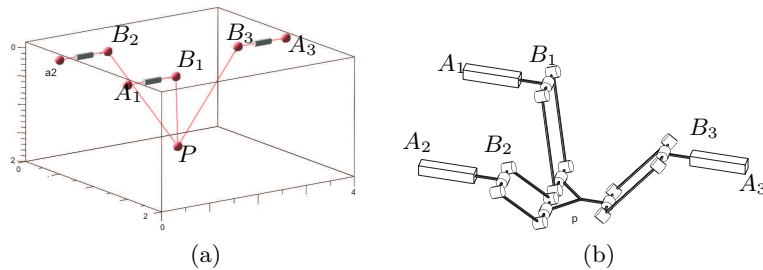


FIGURE 6: Configuration of Triaglide : (a) simplified; (b) real.

As shown in Fig.(6), the *Triaglide* manipulator is driven by three actuated prismatic joints, in which all the three actuators all parallel to each other and placed in the same plane.

The constraint equations for the Triaglide are :

$$\begin{aligned}(x - 1)^2 + (y - \rho_1)^2 + z^2 &= L^2 \\ (x + 1)^2 + (y - \rho_2)^2 + z^2 &= L^2 \\ x^2 + (y - \rho_3)^2 + z^2 &= L^2\end{aligned}\tag{5}$$

#### 405 3.4. *UraneSX Architecture and Kinematics*

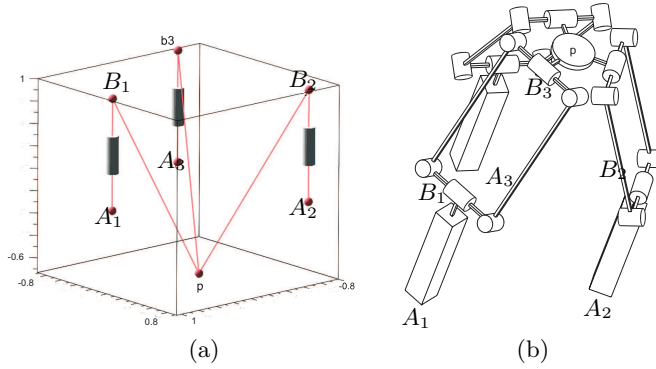


FIGURE 7: Configuration of UraneSX : (a) simplified ; (b) real.

As shown in Fig.(7), the *UraneSX* is similar to triaglide, but instead of three actuators in the same plane, they are placed in different planes. The constraint equations for the UraneSX are :

$$\begin{aligned}(x - 1)^2 + y^2 + (z - \rho_1)^2 &= L^2 \\ (x + 1/2)^2 + (y - \sqrt{3}/2)^2 + (z - \rho_2)^2 &= L^2 \\ (x + 1/2)^2 + (y + \sqrt{3}/2)^2 + (z - \rho_3)^2 &= L^2\end{aligned}\tag{6}$$

#### 4. Singularities : Delta-Like Family Robot

Singularities of a robotic manipulator are important feature that essentially influence its motion capabilities. Mathematically, a singular configuration may be defined as rank deficiency of the Jacobian describing the differential mapping from the joint space to the workspace and vice versa. Differentiating the constraints equations with respect to time leads to the following velocity relationship :

$$\mathbf{A}\mathbf{t} + \mathbf{B}\dot{\mathbf{q}} = 0\tag{7}$$

410 where  $\mathbf{A}$  and  $\mathbf{B}$  are the parallel and serial Jacobian matrices, respectively,  $\mathbf{t}$  is the velocity of  $\mathbf{P}$  and  $\dot{\mathbf{q}}$  joint velocities. The parallel singularities occur whenever  $\det(\mathbf{A}) = 0$ , while the serial singularities occur whenever  $\det(\mathbf{B}) = 0$ .

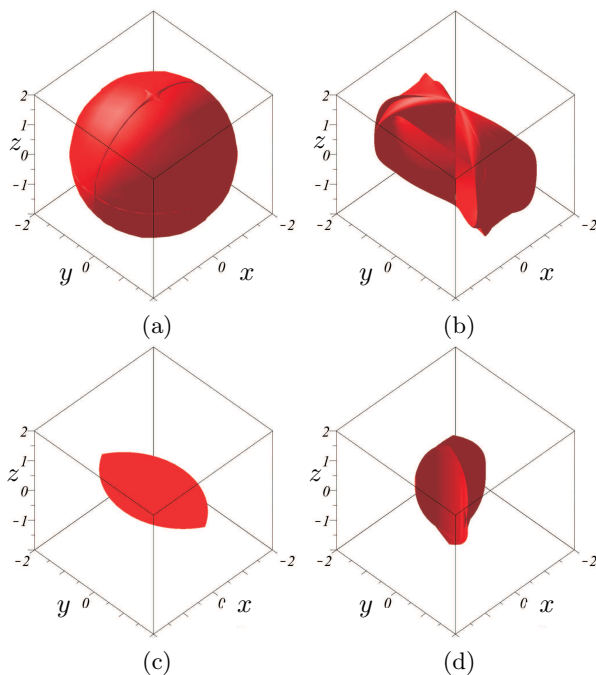


FIGURE 8: Projection of parallel singularity surface in the workspace for (a) Orthoglide, (b) Hybridglide, (c) Triaglide and (d) UraneSX

#### 4.1. Parallel Singularities : Projection in workspace and joint space

Parallel singularities occur when the determinant of the direct kinematics matrix  $\mathbf{A}$  vanishes. The corresponding singular configurations are located inside the workspace. They are particularly undesirable because the manipulator can not resist any force and control is lost. Parallel singularity and its projection surfaces in workspace and joint space are calculated using the function **ParallelSingularities()**. Listing 13 shows an example for calculating the singularity surfaces and its projection in joint space.

```

1 s2      := ParallelSingularities ( robot      :: Manipulator )
2 s2_cart := Projection          ( s2 , robot:-PoseVariables )
3 s2_art  := Projection          ( s2 , robot:-ArticularVariables )

```

Listing 13: Projection of parallel singularity surface of delta-like robot in workspace and joint space

Parallel singularities and their projections in workspace and joint space are computed using a Gröbner based elimination method. This usual way for eliminating variables (see [32]) computes (the algebraic closure of) the projection of the parallel singularities in the workspace.

Eliminating variables can be done in favorable case by using cascading resultants. The main related result says that given two polynomials  $P, Q \in \mathbb{C}[x_1, \dots, x_n]$  and their resultant  $R \in \mathbb{C}[X_1, \dots, x_{n-1}]$  and  $\alpha = (\alpha_1, \dots, \alpha_{n-1}) \in \mathbb{C}$  such that  $R(\alpha) = 0$ , then, either  $\alpha$  cancels the leading terms of  $P, Q$  in  $x_n$

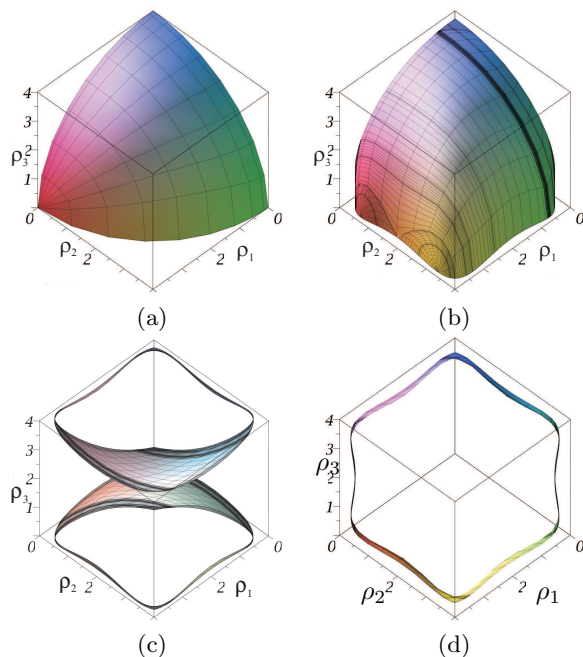


FIGURE 9: Projection of parallel singularity surfaces in the joint space for (a) Orthoglide, (b) Hybridglide, (c) Triaglide and (d) UraneSX

(which means that some parts of the varieties  $P = 0$  or  $Q = 0$  are  $\ll$  going to infinity  $\gg$  or  $\exists \alpha_n \in \mathbb{C}$  such that  $P(\alpha_1, \dots, \alpha_n, \alpha_{n+1}) = Q(\alpha_1, \dots, \alpha_n, \alpha_{n+1}) = 0$ . Some linear change of variables allows to ignore the parts  $\ll$  going to infinity  $\gg$  and  $\{x \in \mathbb{C}^{n-1}, R(x) = 0\}$  is then the projection of  $V(P, Q) = \{x \in \mathbb{C}^n, P(x) = Q(x) = 0\}$ . One can generalize this elimination step to sets of more than two polynomials.

Taking pairs of resultants and computing their resultant with respect to  $x_{n-1}$  one then project again, eliminating one more variable, defining so a cascading process that will finish with univariate polynomials. This process has almost the same complexity as the projection step in a CAD adapted to the input polynomials : at each step, the degree of the polynomials is doubling inducing an exponential growth (double exponential in the number of variables).

On the contrary, in favorable situations (which is our case) the discriminant variety is known to induce a lower growth of coefficients and degrees (single exponential in the number of variables [33]).

Let have a look to the intersection of 3 algebraic surfaces  $p_1(x_1, x_2, x_3) = p_2(x_1, x_2, x_3) = p_3(x_1, x_2, x_3) = 0$  of  $\mathbb{C}^3$  defining a finite set of points. Such a system can also be viewed as the intersection of 3 space curves  $p_1 = p_2 = 0$ ,  $p_1 = p_3 = 0$  and  $p_2 = p_3 = 0$ . By computing the resultant of each pairs of polynomials wrt  $x_3$  one gets the projections of the space curves onto the coordinates  $x_1, x_2$ .

A point is that the intersection of these projections might contain more points than the projection of the intersections of the space curves. It is easy to see that two space curve that do not intersect might have projections with non

empty intersections. The cascading process might follow with the plane curves, but (numerous) spurious points might have been introduced.

$$\begin{aligned}
\det(\mathbf{A})_o &= -\rho_1\rho_2\rho_3 + \rho_1\rho_2z + \rho_1\rho_3y + \rho_2\rho_3x \\
\det(\mathbf{A})_h &= -\rho_1\rho_3x + \rho_2\rho_3x - \rho_1\rho_3 + \rho_1z - \rho_2\rho_3 + \rho_2z + 2\rho_3y \\
\det(\mathbf{A})_u &= \sqrt{3}(3z - \rho_1 - \rho_2 - \rho_3 + \rho_3x + \rho_2x - 2\rho_1x) + 3\rho_3y - 12\rho_2y \\
\det(\mathbf{A})_t &= \rho_1z + \rho_2z - 2\rho_3z
\end{aligned} \tag{8}$$

In the same way, one can compute (the algebraic closure of) the projection of the parallel singularities in the joint space. Both are then defined as the zero set of some system of algebraic equations and we assume that the considered robots are generic enough so that both are hypersurfaces.  $\det(\mathbf{A})_o$ ,  $\det(\mathbf{A})_h$ ,  $\det(\mathbf{A})_t$  and  $\det(\mathbf{A})_u$  are the parallel singularities of Orthoglide, Hybridglide, Triaglide and UraneSX, respectively, as shown in Eq.(8). Starting from the constraint equations and the determinant of the Jacobian matrix, we are able to eliminate the joint values. This elimination strategy is more efficient than a cascading elimination by means of resultants which might introduce many more spurious solutions : singular points that are not projections of singular points.

Figure (9) shows the projections of singularity surface  $s2$  in joint space and  $s2\_art$  is the projection surface. And  $s2\_art$  is the projection curve in workspace shown in Fig.(8).

#### 4.2. Serial Singularities : Projection in workspace and joint space

Serial singularities occur when the determinant of the inverse kinematics matrix  $\mathbf{B}$  vanishes. When the manipulator is in such a singularity, there is a direction along which no Cartesian velocity can be produced. Serial singularity analysis of delta-like robot is done using the function **SerialSingularities()** shown in Listing 14.

```

1 s1      := SerialSingularities( robot      :: Manipulator      )
2 s1_cart := Projection          ( s1, robot:-PoseVariables    )
3 s1_art  := Projection          ( s1, robot:-ArticularVariables)

```

Listing 14: Projection of serial singularities in workspace and joint space

In Eq.(9),  $\det(\mathbf{B})_o$ ,  $\det(\mathbf{B})_h$ ,  $\det(\mathbf{B})_t$  and  $\det(\mathbf{B})_u$  are the serial singularities of Orthoglide, Hybridglide, Triaglide and UraneSX, respectively. One can compute (the algebraic closure of) the projection of the serial singularities in the joint space and workspace. Both are then defined as the zero set of some system of algebraic equations and we assume that the considered robots are generic enough so that both are hypersurfaces. Also these surfaces are shown in Fig.(10) and Fig.(11).

$$\begin{aligned}
\det(\mathbf{B})_o &= (\rho_1 - x)(\rho_2 - y)(\rho_3 - z) \\
\det(\mathbf{B})_h &= (\rho_1 - y)(\rho_2 - y)(\rho_3 - z) \\
\det(\mathbf{B})_u &= (\rho_1 - z)(\rho_2 - z)(\rho_3 - z) \\
\det(\mathbf{B})_t &= (\rho_1 - y)(\rho_2 - y)(\rho_3 - y)
\end{aligned} \tag{9}$$



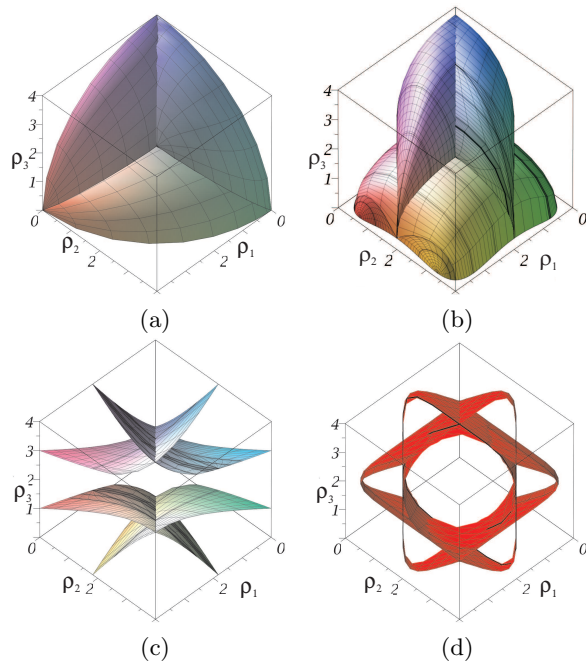


FIGURE 10: Projection of serial singularity surfaces in the joint space for (a) Orthoglide, (b) Hybridglide, (c) Triaglide and (d) UraneSX

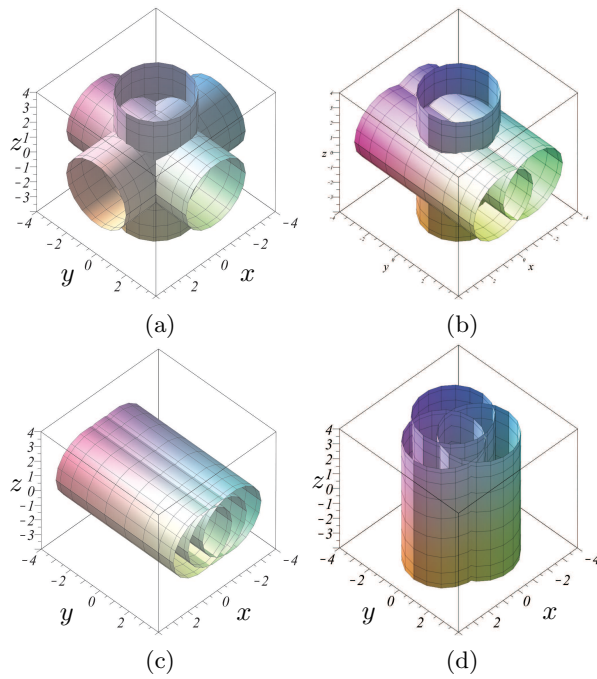


FIGURE 11: Projection of serial singularity surfaces in the workspace for (a) Orthoglide, (b) Hybridglide, (c) Triaglide and (d) UraneSX

Figure (10) shows the projections of singularity surface  $s1$  in joint space and  $s1_{art}$  is the projection surface. And  $s1_{cart}$  is the projection surface in workspace and is shown in Fig.(11).

#### 490 4.3. Complexity in Singularities

In Table 3 and 4, a comparative study of five parameters among the family of delta like robot is presented. We have tabulated the main characteristics of the polynomials (In three variables) used for the plots (Implicit surface) : their total degree, their number of terms and the maximum bitsize of their coefficients. We  
 495 have also reported the time (In seconds) for plotting the implicit surface which they define and the number of cells computed by the CAD, as well as the number of plotted cells where the equations admits real solutions in the plotted range.

This function is more precise than Maple’s “implicitplot3d” function because it calculates all the singular places of the surface and then triangulates it. The  
 500 surface is not calculated only a discretization of the space. Several functions are used which involves the discriminant variety, Gröbner bases and CAD computations, computed in Maple 2018 with a Intel(R) Core(TM) i7-5600U CPU 2.60 GHz (16 Gb RAM). As can be seen from Table 3, there exists higher values of all the parameters for the Hybridglide, among all manipulators listed, which infers that it has more complex parallel singularities, whereas for the Triaglide all the  
 505 values are least which intuits the less complicated singularities. For example, the computation times for the Hybridglyde for parallel singularities is high compared to the one for the Othoglide, even if the surface has similar characteristics. This is due to the geometry of the surface which is more difficult to decompose in the case of the Hybridglide : the CAD is described by 636 cylindrical cells in the case of Hybridglide while it is described by 300 cells for the Orthoglide because a large part of the singularity surface is a sphere.

From Table 4, it can be inferred that there exists higher values of all the parameters for the UraneSX, among all manipulators listed, which infers that it  
 515 has more complex serial singularities, whereas for the Triaglide all the values are least which intuits the less complicated singularities. The computation times for plotting the serial singularities in joint space is higher compared to others.

## 5. Workspace Analysis of a Delta-like Family Robot

The workspace analysis allows to characterize of the workspace regions where  
 520 the number of real solutions for the inverse kinematics is constant. A CAD algorithm is used to compute the workspace of the robot in the projection space  $(x, y, z)$  with some joint constraints (shown in Eq. 2) taken in account.

The three main steps involved in the analysis are [17, 26, 34] :

- Computation of a subset of the joint space (resp. workspace) where the  
 525 number of solutions changes : the *Discriminant Variety* .
- Description of the complementary of the discriminant variety in connected cells : the Generic CAD.
- Connecting the cells belonging to the same connected component in the counterpart of the discriminant variety : *interval comparisons*.

530 Table 5 shows the number of cells corresponding to the number of solutions in the workspace, which is the outcome of cell decomposition. The different

TABLE 3: Comparison of the different parameters associated with the projection of parallel singularity surface in the workspace and joint space for the delta-like robots

PARALLEL SINGULARITIES					
Projection in Workspace					
Manipulators	Plotting Time	Degrees	No.of terms	Binary	No. of Cells
Orthoglide	07.650	18[10,10,10]	097	015	[0300,42]
Hybridglide	23.536	20[16,08,12]	119	017	[0636,80]
Triaglide	13.682	03[00,00,03]	002	002	[0150,04]
UraneSX	25.100	06[06,04,00]	015	040	[2795,66]
Projection in Joint Space					
Orthoglide	00.850	06[04,04,04]	010	004	[012,01]
Hybridglide	02.917	06[04,04,04]	025	006	[111,20]
Triaglide	09.589	06[04,04,04]	041	006	[126,51]
UraneSX	02.300	06[04,04,04]	041	051	[041,09]

TABLE 4: Comparison of the different parameters associated with the projection of serial singularity surface in the workspace and joint space for the delta-like robots

SERIAL SINGULARITIES					
Projection in Workspace					
Manipulators	Plotting Time	Degrees	No.of terms	Binary	No. of Cells
Orthoglide	07.230	06[04,04,04]	017	006	[016,02]
Hybridglide	07.243	06[06,02,04]	015	006	[045,03]
Triaglide	05.437	06[06,06,00]	010	006	[045,03]
UraneSX	10.700	06[12,12,00]	013	036	[045,03]
Projection in Joint Space					
Orthoglide	03.957	18[12,12,12]	062	012	[021,03]
Hybridglide	06.173	18[12,12,12]	281	017	[158,27]
Triaglide	06.794	06[06,06,06]	042	007	[077,17]
UraneSX	07.400	12[12,12,12]	252	151	[108,29]

TABLE 5: Definition of the Workspace with CAD

Workspace : Number of cells						
Number of solutions	0	1	2	4	8	Total
Orthoglide	28782	1196	0	0	130	30108
Hybridglide	93292	4484	7228	4196	1164	110364
Triaglide	27708	384	464	420	400	29376
UraneSX	9918	236	36	0	0	10190

535 shapes of workspace for the delta-like robots is shown in Fig.(12), where blue, red, yellow and green regions correspond to the one, two, four and eight number of solutions for the IKP. A comparative study is done on the workspace of the family of delta-like manipulator and the results are shown in Fig.(12). All the

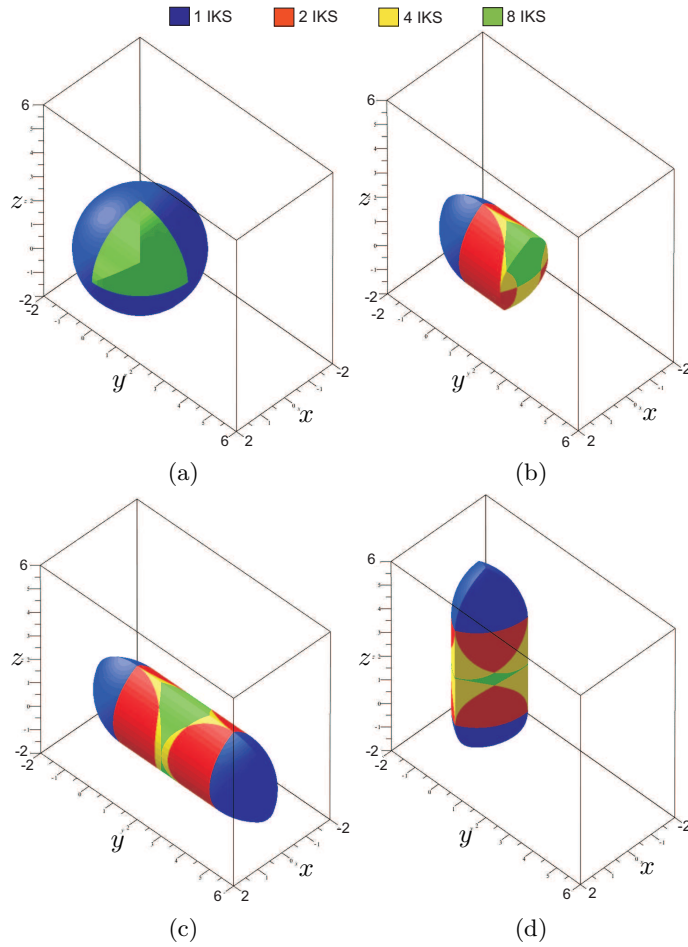


FIGURE 12: Workspace plot for Orthoglide (a), Hybridglide (b), Triaglide (c) and UraneSX (d) robot

workspace are plotted in the rectangular box, where  $x \in [-2, 2]$ ,  $y \in [-2, 6]$  and  $z \in [-2, 6]$ , so that the shapes of these workspace can be compared. From the Fig. 12 it can be intuited that the Triaglide will be good selection, if the task space is more in horizontal plane, whereas the Orthoglide is good for the three dimensional task space.

The number of cells in the workspace plays a role in motion generation when one want to know if a path is in the workspace [35]. Indeed, if we discretize the path, a Maple function named "CellLocation" allows us to know where an pose is located from the list of cells calculated with the CAD.

## 6. Joint space Analysis of a Delta-like Family Robot

The Joint space analysis predicts the feasible and non-feasible combinations of the prismatic joint variables which are essential for the parallel robot control. The boundaries of the joint space are either the surfaces associated with the

parallel singularities or the surfaces associated with the joint limits. The Joint  
 550 space analysis is done using CAD using the joint limits defined in Eq. 2. These  
 cells are plotted in Fig. (13) where red region corresponds to two solutions for the  
 DKP. One can note that for the Orthoglide and Hybridglide robots, the shape  
 of the joint space is regular and composed of a single connected component. For  
 Triaglide and UraneSX robots, the joint space consists of several components  
 555 either completely disconnected or connected by single lines. If we want to define  
 a robot with simple joint boundaries (defined by intervals), Orthoglide and  
 Hybridglide robots will be the best selections.

Table 6 shows the number of cells corresponding to the number of solutions in  
 the joint space, which is the outcome of cell decomposition. The number of cells  
 560 in the joint space plays an important part while simulating robot movements  
 when control or robot geometry errors are introduced into the model. A path  
 that can be achieved in the workspace may be too close to singular configurations  
 after the use of the inverse geometric model including these disturbances [35].  
 The “CellLocation” Maple function can be used to evaluate the position of the  
 articular trajectory.

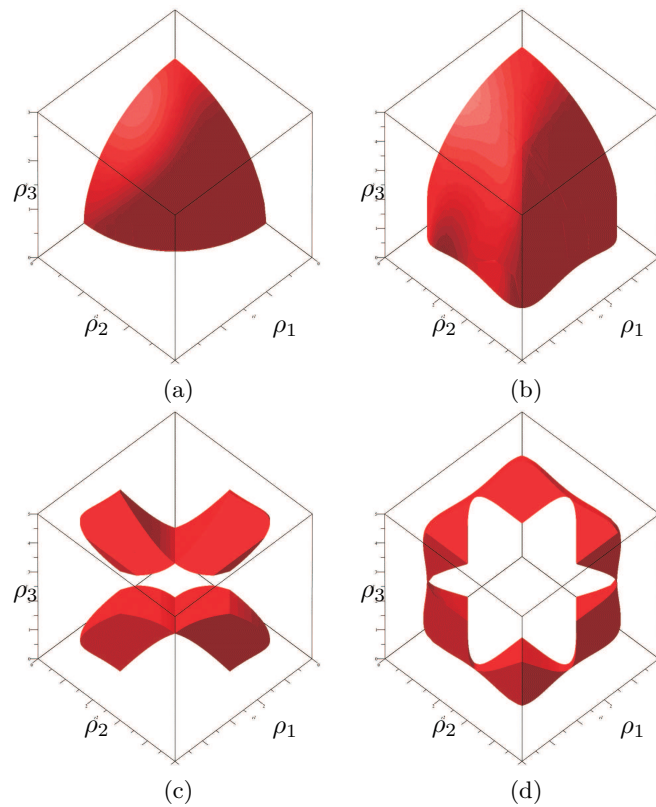


FIGURE 13: Joint space plot for Orthoglide (a), Hybridglide (b), Triaglide (c) and UraneSX (d) robot

565

TABLE 6: Definition of the Joint space with CAD

Joint space : Number of cells						
Number of solutions	0	1	2	4	8	Total
Orthoglide	10509	0	4160	0	0	14669
Hybridglide	98917	0	3041	0	0	11958
Triaglide	5375	0	426	0	0	5801
UraneSX	50598	0	4006	0	0	54604

## 7. Conclusions

A comparative study on the workspace of different delta-like robots gives the idea about the shape of the workspace, which further plays an important role in the selection of the manipulator for the specific task or for the trajectory planning. The main characteristics associated with the singularities are tabulated in Table 4 and 3, which also gives some information about the complexity of the singularities, which is an essential factor for the singularity-free path plannings. From these data, it can be observed that the singularities associated with the Hybridglide are complicated, whereas the structure of those associated with the Triaglide is rather simple. For the Orthoglide and Hybridglide robots, the shape of the joint space is regular and composed of a single connected component, whereas for Triaglide and UraneSX robots, the joint space consists of several components either completely disconnected or connected by single lines.

- [1] Y. Tsai, A. Soni, An algorithm for the workspace of a general nr robot, *Journal of Mechanisms, Transmissions, and Automation in Design* 105 (1) (1983) 52–57.
- [2] J. A. Hansen, K. Gupta, S. Kazerounian, Generation and evaluation of the workspace of a manipulator, *The International Journal of Robotics Research* 2 (3) (1983) 22–31.
- [3] C. Gosselin, Determination of the workspace of 6-dof parallel manipulators, *ASME Journal of Mechanical Design* 112 (3) (1990) 331–336.
- [4] J.-P. Merlet, Geometrical determination of the workspace of a constrained parallel manipulator, *Advances in Robot Kinematics*, Ferrare, Italy, Sept (1992) 7–9.
- [5] G. Castelli, E. Ottaviano, M. Ceccarelli, A fairly general algorithm to evaluate workspace characteristics of serial and parallel manipulators, *Mechanics based design of structures and machines* 36 (1) (2008) 14–33.
- [6] I. A. Bonev, J. Ryu, A new approach to orientation workspace analysis of 6-dof parallel manipulators, *Mechanism and machine theory* 36 (1) (2001) 15–28.
- [7] D. Chablat, P. Wenger, F. Majou, J.-P. Merlet, An interval analysis based study for the design and the comparison of three-degrees-of-freedom parallel kinematic machines, *The International Journal of Robotics Research* 23 (6) (2004) 615–624.

- 600 [8] M. Zein, P. Wenger, D. Chablat, An exhaustive study of the workspace topologies of all 3r orthogonal manipulators with geometric simplifications, *Mechanism and Machine Theory* 41 (8) (2006) 971–986.
- [9] E. Ottaviano, M. Husty, M. Ceccarelli, Identification of the workspace boundary of a general 3-r manipulator, *Journal of Mechanical Design* 605 128 (1) (2006) 236–242.
- [10] D. Chablat, R. Jha, F. Rouillier, G. Moroz, Non-singular assembly mode changing trajectories in the workspace for the 3-rps parallel robot, in : *Advances in Robot Kinematics*, Springer, 2014, pp. 149–159.
- [11] D. Chablat, G. Moroz, P. Wenger, Uniqueness domains and non singular assembly mode changing trajectories, in : *Robotics and Automation (ICRA)*, 2011 IEEE International Conference on, IEEE, 2011, pp. 3946–3951. 610
- [12] R. Jha, Contributions to the performance analysis of parallel robots, Ph.D. thesis, Ph. D. Thesis, École Centrale de Nantes (2016).
- [13] B. Siciliano, O. Khatib, *Springer handbook of robotics*, Springer, 2016.
- 615 [14] J. Snyman, L. Du Plessis, J. Duffy, An optimization approach to the determination of the boundaries of manipulator workspaces, *Journal of Mechanical Design* 122 (4) (2000) 447–456.
- [15] I. A. Bonev, C. M. Gosselin, Analytical determination of the workspace of symmetrical spherical parallel mechanisms, *IEEE Transactions on Robotics* 620 22 (5) (2006) 1011–1017.
- [16] O. Bohigas, M. Manubens, L. Ros, A complete method for workspace boundary determination on general structure manipulators, *IEEE Transactions on Robotics* 28 (5) (2012) 993–1006.
- 625 [17] D. Chablat, R. Jha, F. Rouillier, G. Moroz, Workspace and joint space analysis of the 3-rps parallel robot, in : *ASME 2014 International Design Engineering Technical Conferences and Computers and Information in Engineering Conference*, American Society of Mechanical Engineers, 2014, pp. V05AT08A056–V05AT08A056.
- [18] R. Jha, D. Chablat, F. Rouillier, G. Moroz, Workspace and singularity analysis of a delta like family robot, in : *Robotics and Mechatronics*, Springer, 630 2016, pp. 121–130.
- [19] R. Jha, D. Chablat, L. Baron, Influence of design parameters on the singularities and workspace of a 3-rps parallel robot, *Transactions of the Canadian Society for Mechanical Engineering* 42 (1) (2018) 30–37.
- 635 [20] P. Wenger, D. Chablat, Kinetostatic analysis and solution classification of a planar tensegrity mechanism, in : *Computational Kinematics*, Springer, 2018, pp. 422–431.
- 640 [21] G. Moroz, F. Rouiller, D. Chablat, P. Wenger, On the determination of cusp points of 3-rpr parallel manipulators, *Mechanism and Machine Theory* 45 (11) (2010) 1555–1567.

- [22] M. Manubens, G. Moroz, D. Chablat, P. Wenger, F. Rouillier, Cusp points in the parameter space of degenerate 3-rpr planar parallel manipulators, *Journal of mechanisms and robotics* 4 (4) (2012) 041003.
- [23] G. Moroz, D. Chablat, P. Wenger, F. Rouillier, Cusp points in the parameter space of rpr-2pr parallel manipulators, in : *New Trends in Mechanism Science*, Springer, 2010, pp. 29–37.
- [24] S. Caro, P. Wenger, D. Chablat, Non-singular assembly mode changing trajectories of a 6-dof parallel robot, in : *ASME 2012 International Design Engineering Technical Conferences and Computers and Information in Engineering Conference*, American Society of Mechanical Engineers, 2012, pp. 1245–1254.
- [25] J.-P. Merlet, *Parallel robots*, Vol. 128, Springer Science & Business Media, 2006.
- [26] D. Lazard, F. Rouillier, Solving parametric polynomial systems, *Journal of Symbolic Computation* 42 (6) (2007) 636–667.
- [27] J. Gerhard, D. Jeffrey, G. Moroz, A package for solving parametric polynomial systems, *ACM Communications in Computer Algebra* 43 (3/4) (2010) 61–72.
- [28] Maple, *Cylindrical Algebraic Decomposition*, Vol. Maple User Manual, Toronto : Maplesoft, a division of Waterloo Maple Inc., 2005-2015.
- [29] Maple, *Cell Decomposition*, Vol. Maple User Manual, Toronto : Maplesoft, a division of Waterloo Maple Inc., 2005-2015.
- [30] A. Pashkevich, D. Chablat, P. Wenger, Kinematics and workspace analysis of a three-axis parallel manipulator : the orthoglide, *Robotica* 24 (1) (2006) 39–49.
- [31] M. Hebsacker, T. Treib, O. Zirn, M. Honegger, Hexaglide 6 dof and triaglide 3 dof parallel manipulators, in : *Parallel kinematic machines*, Springer, 1999, pp. 345–355.
- [32] D. A. Cox, J. Little, D. O’shea, *Using algebraic geometry*, Vol. 185, Springer Science & Business Media, 2006.
- [33] G. Moroz, Properness defects of projection and minimal discriminant variety, *Journal of Symbolic Computation* 46 (10) (2011) 1139–1157.
- [34] G. Moroz, *Sur la décomposition réelle et algébrique des systèmes dépendant de paramètres*, Ph.D. thesis, Université Pierre et Marie Curie-Paris VI (2008).
- [35] R. Jha, D. Chablat, F. Rouillier, G. Moroz, An algebraic method to check the singularity-free paths for parallel robots, in : *ASME 2015 International Design Engineering Technical Conferences and Computers and Information in Engineering Conference*, American Society of Mechanical Engineers, 2015, pp. V05CT08A002–V05CT08A002.